Hindawi
Advances in Meteorology
Volume 2019, Article ID 1353195, 12 pages
https://doi.org/10.1155/2019/1353195

Research Article

Fractal Analysis of the Long-Term Memory in Precipitation over Bénin (West Africa)

Medard Noukpo Agbazo,[1] **Gabin Koto N'Gobi**,[2] **Eric Alamou**,[3] **Basile Kounouhewa**,[2] **and Abel Afouda**[3]

[1]*International Chair in Physics Mathematics and Applications (CIPMA-Chair Unesco), University of Abomey-Calavi, Abomey-Calavi BP: 526 UAC, Benin*
[2]*Laboratoire de Physique du Rayonnement (LPR), University of Abomey-Calavi, Abomey-Calavi BP: 526 UAC, Benin*
[3]*Laboratoire d'Hydrologie Appliquée (LHA), University of Abomey-Calavi, Abomey-Calavi BP: 526 UAC, Benin*

Correspondence should be addressed to Medard Noukpo Agbazo; agbazomedard@yahoo.fr

Received 30 September 2018; Accepted 19 December 2018; Published 9 January 2019

Academic Editor: Anthony R. Lupo

This study analyzed the long-term memory (LTM) in precipitation over Bénin synoptic stations from 1951 to 2010 using the detrended fluctuation analysis (DFA) method. Results reveal the existence of positive long-term memory characteristic in rainfall field. DFA exponent values are different regarding the concerned synoptic stations, reflecting the effect of geographical position and climate on the LTM. These values were related to the type of climate. The best DFA1-4 method depends on the geographical position of the studied station. However, DFA2 is generally the best in terms of spatial average from DFA1 to DFA4. In Bénin synoptic stations, except the Parakou station, the long-term temporal correlations are systematically the source of multifractality in rainfall. Except Natitingou, the strength of long-term memory characteristic decreases each twenty years in the study period. Considering the fractal approach, our results show that the subperiod 1991–2010 is not really a transition period as shown before. Thus, the drought is prolonging until 2010. So, fractal theory reveals more Bénin climatic characteristics.

1. Introduction

According to several reports, such as those of the United Nations Framework Convention on Climate Change [1], the International Panel of Climate Change (IPCC) [2], several documents produced by the World Bank [3], and the Climate Change and Urban Vulnerability in Africa (CLUVA) project [4], Africa is considered as a continent particularly vulnerable to climate change. But, the real impact, especially on a local scale, is still poorly understood. Changes in climate have significant implications for societies, future generations, the economy, ecosystems, and agriculture [5]. Moreover, climate change has the self-memory characteristic [6]. This self-memory characteristic is widely known as long-range correlation (also called the long-term memory, LTM). So, a better understanding of long-term climate memory by improved methods is very important for predicting climate change in Africa. This would significantly reduce the vulnerability and prepare populations for climate change adaptation. Also, this understanding can help to understand more, a complex dynamic behavior in climate effects. Climate change is marked with variation in precipitations [7]. Long-term memory exists in precipitation records [8–11]. Precipitation memory characteristics have been widely studied in various regions of the world. For instance, Kantelhardt et al. [9] have studied, by the detrended fluctuation analysis (DFA) method, the LTM characteristics of precipitation records in Europe, Asia, and America. In Africa, Efstathiou and Varotsos [12] have applied the DFA method to explore the intrinsic properties of Sahel precipitation anomalies. They found that the fluctuations of the precipitation anomalies in small time intervals are positively correlated to those in longer time intervals in a power law fashion [12]. According to Taqqu et al. [13] and Kantelhardt et al. [9], the DFA method permits to

estimate the Hurst exponent H. It is important to remind the distinction of the classic Hurst and the DFA exponent as announced in Taqqu et al. [13], Movahed et al. [14, 15], and more recently as clarified by Hall [16] and Varotsos and Efstathiou [17]. According to Hall [16] and Varotsos and Efstathiou [17], the relationship between the DFA exponent and the classic Hurst exponent H can be expressed as (i) for fractional Gaussian noise (fGn), H is equal to DFA exponent and (ii) for fractional Brownian motions (fBm), H is equal to DFA exponent 1. Moreover, for fGn processes (which is a stationary process), 0 < DFA exponent < 1 and for fBm processes (which is nonstationary process), 1 < DFA exponent < 2 [16]. The estimation of such exponent from a given dataset is an effective way to detect the LTM characteristics in it. However, Maraun et al. [18] and Varotsos and Efstathiou [17] suggested that two criteria are needed to ensure the existence of the long-range correlation: (i) the rejection of the simple exponential decay of the autocorrelation function and (ii) the establishment of the power law scaling. Although some claim that the DFA exponent or Hurst exponent H is not universal for meteorological and climatological data [19, 20], precipitation have characteristic values of DFA exponent or Hurst exponent H [21, 22]. One can be sure of the universality of the correlations in climatological time series but its DFA exponents can be related to local patterns.

Bénin is one of the West Africa countries affected by the effects of climate change [3]. Long-term memory of precipitation is not yet studied in fractal framework in Bénin. In the literature, it has been shown that long-range correlations in weather and climate systems depend on geographical locations [11]. It is important to find out what is the long-term memory of precipitation at Bénin meteorological synoptic stations located in two main climatic areas (subequatorial climate and Sudanian climate).

The purpose of this paper is to study, for the first time in Bénin, the long-term memory of precipitation. The paper is organized as follows: in Section 2, the method of DFA and the dataset are described. Analysis of results and their interpretations are made in Section 3. Discussion of results is made in Section 4. Finally, we conclude the paper with a summary and outlook for further research in Section 5.

2. Materials and Methods

2.1. Materials

2.1.1. Site Description. The study covers all the synoptic stations of Bénin, the geographical positions of which are shown in (Figure 1). Bénin is characterized from the South to North by three climatic zones in which stations are located [23]: Cotonou, Bohicon, and Savè are located in the subequatorial region where March is the hottest month (~26°C), while August is the coldest month (~24°C). The daily and annual thermal amplitudes are, respectively, ~10°C and ~5°C. The relative humidity ranges between 70% and 95% because of the proximity to the Atlantic Ocean. The subequatorial climate has four seasons: a long rainy season (April to July) followed by a short dry season (August to September) and a short rainy season (October to November) followed by long dry season (December to March) in the year. However, the stations of Parakou, Kandi, and Natitingou are located in Sudanian region in the northern part of the country. The daily mean of air temperatures in Natitingou, Parakou, and Kandi are, respectively, ~25°C, ~27°C, and ~35°C. Parakou and Savè are located in the transition area between the two kinds of climatic zone.

2.1.2. Data Records. Data were provided by the Agency for the Aerial Navigation's Security in Africa and in Madagascar (ASECNA). Daily rainfall data from Bénin synoptic stations are used during a period from 1951 to 2010. Rainfall variation during the study period is presented in Figure 2 for each synoptic station.

2.2. Methods

2.2.1. Description of the MFDFA Method. The multifractal detrended fluctuation analysis (MFDFA) method is a generalization of the standard DFA method. It is generally preferred and widely used in the literature to detect the fractal scaling properties of the mth-order moments and long-term memory in nonstationary and nonlinear time series as, meteorological and climatological series [6, 24, 25]. The modified MFDFA procedure consists of a sequence of steps and detailed information about computation can be found in [26]. The steps are essentially identical to the conventional DFA procedure. It can be briefly described as follow [6].

Let $\{x_t \mid t = 1, 2, \ldots, N\}$ be an original time series of N equidistant measurements to which the procedure of the DFA method is applied. First, a news series named "profile" is determined as follows:

$$Y(k) = \sum_{t=1}^{k} (x_t - \langle x \rangle), \tag{1}$$

where $\langle x \rangle$ is the mean value of x_t and $k = 1, 2, \ldots, N$.

The profile is then divided into $N = \text{int}(N/s)$ equal-sized nonoverlapping windows with a length s. Since N is not the integral multiple of s in most cases, there might be a short part at the end of the profile that remains uncovered. To take full account of the series, the same procedure can be repeated starting from the end of the series. Hence, we can obtain $2N_s$ segments altogether. We then calculate the variance of each window as

$$F^2(\nu, s) = \begin{cases} \dfrac{1}{s} \displaystyle\sum_{i=1}^{s} \left\{ Y_{[(\nu-1)s+i]} - y_\nu^{(m)}(i) \right\}^2, \\ \quad \text{for } \nu = 1, 2, \ldots, N_s, \\ \dfrac{1}{s} \displaystyle\sum_{i=1}^{s} \left\{ Y_{[N-(\nu-N_s)s+i]} - y_\nu^{(m)}(i) \right\}^2, \\ \quad \text{for } \nu = (N_s + 1), \ldots, 2N_s. \end{cases} \tag{2}$$

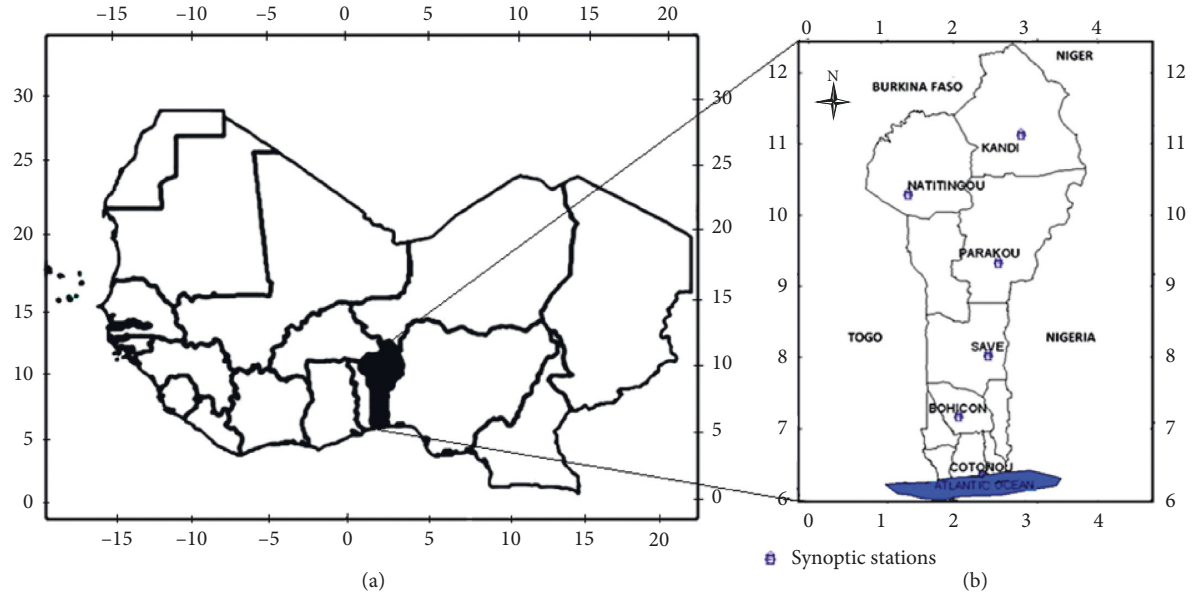

Figure 1: Study sites location: (a) Bénin location in West Africa; (b) synoptic station locations in Bénin.

It should be noted that linear (i.e., polynomial order $m = 1$), quadratic (i.e., $m = 2$), cubic (i.e., $m = 3$), or higher-order polynomials $y_\nu^{(m)}(i)$ can be used to fit the local trend, and MFDFA is noted as MFDFA1, MFDFA2, MFDFA3, MFDFA4, etc. In MFDFAm, possible m order trends are eliminated in the profile. By averaging over all windows, we obtain the fluctuation as

$$F_q(s) = \begin{cases} \left\{ \dfrac{1}{2N_s} \displaystyle\sum_{\nu=1}^{2N_s} \left[F^2(\nu, s)\right]^{q/2} \right\}^{1/q}, & \text{for } q \neq 0, \\ \exp\left\{ \dfrac{1}{4N_s} \displaystyle\sum_{\nu=1}^{2N_s} \ln\left[F^2(\nu, s)\right] \right\}, & \text{for } q = 0. \end{cases} \tag{3}$$

If the time series follows the power law, then we can obtain the scaling function:

$$F_q(s) \propto s^{h(q)}, \tag{4}$$

where $h(q)$ is the generalized Hurst scaling function [9, 27]. In particular, $h(2)$ is the DFA exponent. It is very important to keep in mind the distinction between the classic Hurst and the DFA exponent as indicated earlier in the introduction. According to Hall [16] and Varotsos and Efstathiou [17], $h(2) = H$ for fractional Gaussian noise (fGn) and $h(2) = H + 1$ for fractional Brownian motions (fBm). For $q = 2$, we have the standard DFA analysis and *DFA1*, *DFA2*, *DFA3*, and *DFA4* are corresponding to *MFDFA1*, *MFDFA2*, *MFDFA3*, and *MFDFA4* (i.e., for an m-order DFA process, an m-order polynomial is used to calculate the local trend in each segment). In this case, the scaling exponent $h(2)$ provides information about the average fluctuation of the series. The series can be categorized into one of the following three types depending on the $h(2)$ values. These are (i) $0 < h(2) < 0.5$ for an antipersistent type long-range correlated process (negative long-term memory) where large values (compared to the average) are more likely followed by small values and vice versa, (ii) $h(2) = 0.5$ for an entirely random uncorrelated distribution, and (iii) $0.5 < h(2) < 1$ for a persistent and long-range correlated process (positive long-term memory) where large values are more likely to be followed by large values and vice versa. In this study, $h(2)$ is represented by h.

2.2.2. The Best DFA Method. In order to choose the best DFA method, we have calculated the difference between the h values of two successive orders as follows:

$$\Delta h^{m,m+1} = |h(\text{DFA}m) - h(\text{DFA}m + 1)|, \tag{5}$$

where $h(\text{DFA}m)$ and $h(\text{DFA}m + 1)$ are, respectively, the h values obtained by DFAm and DFA$m + 1$ ($m = 1, 2$ and 3). The DFAm method minimizing $\Delta h^{m,m+1}$ spatially averaged is then used as the best method.

2.2.3. Origins of Multifractality. Generally, there are two types of source of multifractality in time series. One is due to different long-term temporal correlations for small and large fluctuations; the other is due to the fat-tailed distributions of variations [26, 28, 29]. The main methods to find the contributions of the two sources of multifractality are the shuffling procedure and the surrogating procedure, respectively [30]. The shuffling procedure destroys any temporal correlations in the data, but the distributions remain exactly the same. In order to quantify the influence of the broad probability density function, surrogate time series were generated from the original by randomizing their phases in Fourier space, so that the surrogate series are Gaussian. The shuffling procedure consists of generating a random permutation of the array elements of time series. In this paper, we use the common method of amplitude adjusted Fourier transform (AAFT) developed in

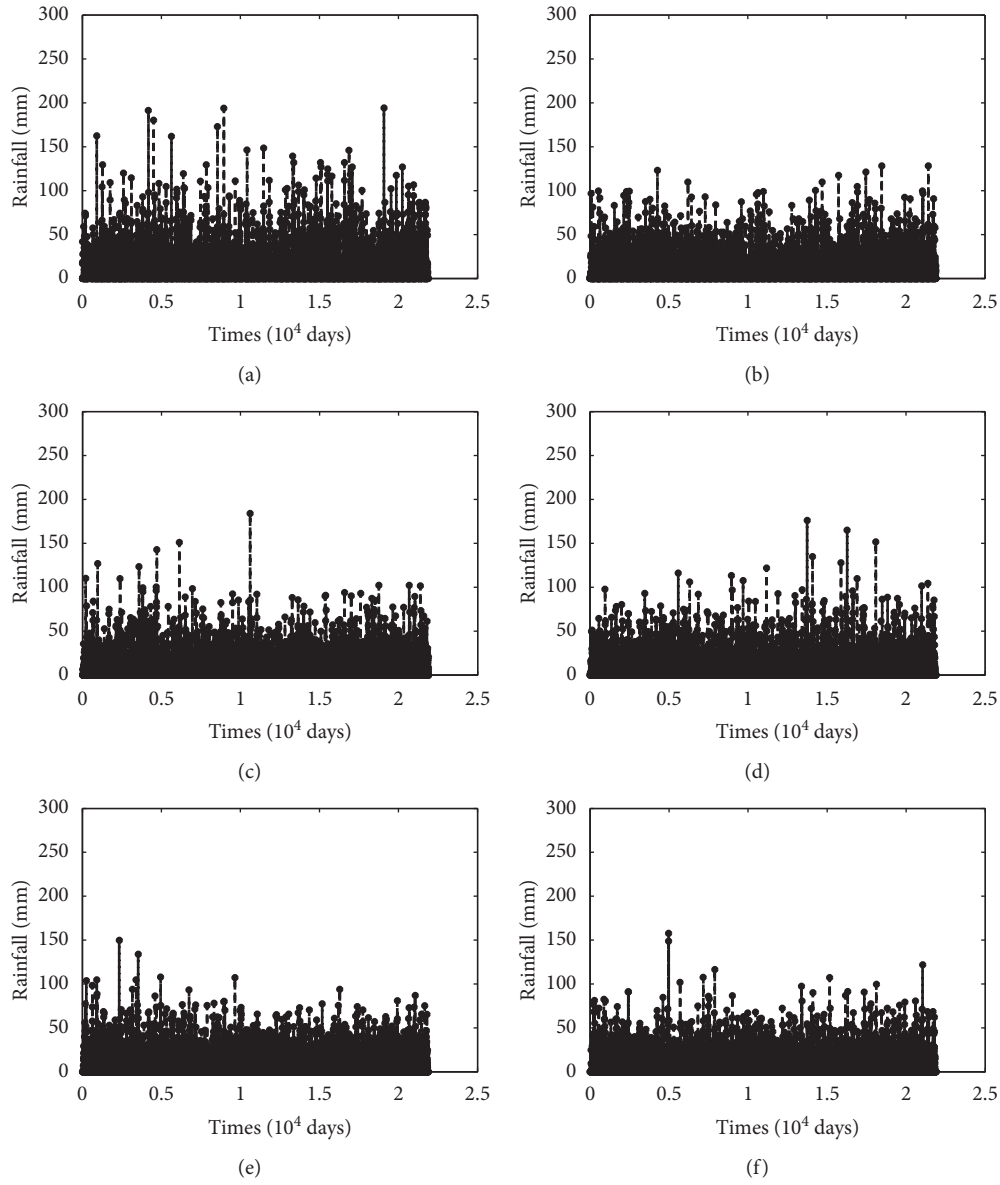

Figure 2: Temporal variations of rainfall time series collected from 1951 to 2010: (a) Cotonou station, (b) Bohicon station, (c) Savè station, (d) Parakou station, (e) Natitingou station, and (f) Kandi station.

[31–33] to obtain surrogates data. AAFT can be summarized according to Dong et al. [32] as follows: (1) a discrete Fourier transform of the original series is conducted, (2) the discrete Fourier transform of the data is multiplied by random phases, and (3) an inverse Fourier transform is performed to generate a phase randomized surrogate. For convenience, $h^{\text{orig}}(q)$, $h^{\text{shuf}}(q)$, and $h^{\text{surr}}(q)$ denote the generalized Hurst scaling function obtained by the best MFDFAm corresponding to the best DFAm for the original, shuffled, and surrogated times series, respectively. In order to avoid a divergence of moments in the fat tails of the fluctuation distribution as mentioned by some authors [34, 35], we restrict the order q within the range $-3 \le q \le 3$ as in [34]. To better compare the impact of both types of multifractality in time, these following computations are done:

$$\begin{aligned} \left|h_{\text{CORR}}(q)\right| &= \left|h^{\text{shuf}}(q) - h^{\text{orig}}(q)\right|, \\ \left|h_{\text{PDF}}(q)\right| &= \left|h^{\text{surr}}(q) - h^{\text{orig}}(q)\right|. \end{aligned} \tag{6}$$

The long-term temporal correlations have a slightly greater effect on multifractality than the broad probability density function, if $|h_{\text{CORR}}(q)| > |h_{\text{PDF}}(q)|$; otherwise, $|h_{\text{CORR}}(q)| < |h_{\text{PDF}}(q)|$. However, nonzero values of $|h_{\text{CORR}}(q)|$ and $|h_{\text{PDF}}(q)|$ indicate that both of them influence the multifractality.

2.2.4. Assessment to Climate Change Effect by the DFA Method. To determine whether changes in the dynamics of rainfall time series can be assessed with the DFA method, the 60 years of data were divided into three separate datasets, the

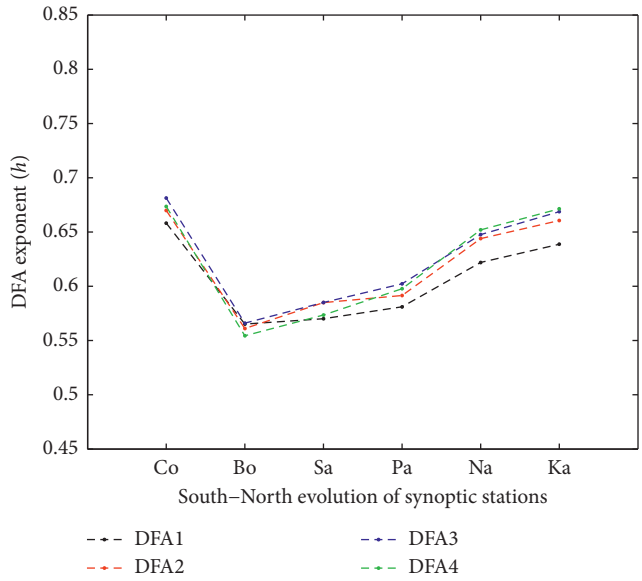

FIGURE 3: South-North distribution of DFA exponents (h) obtained by the *DFA1-4* method. Cotonou (Co), Bohicon (Bo), Savè (Sa), Parakou (Pa), Natitingou (Na), and Kandi (Ka). For a DFAm, an m-order polynomial is used to calculate the local trend in each segment.

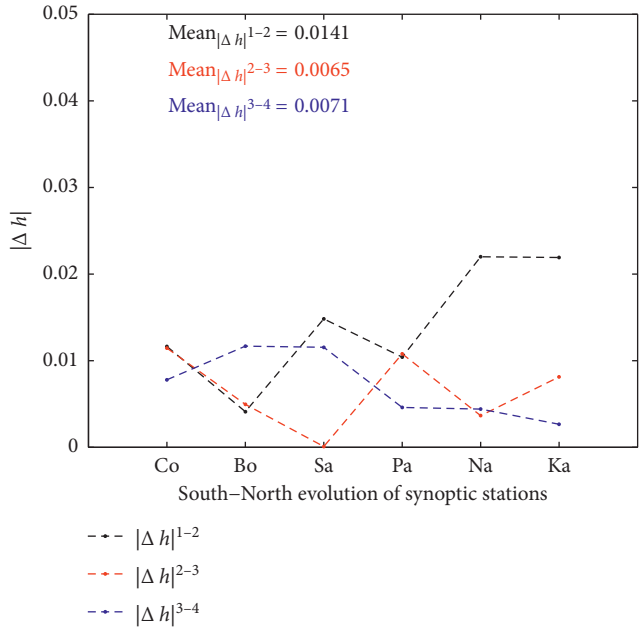

FIGURE 4: Spatial distribution of $\Delta h^{m,m+1}$ obtained by the *DFA1-4* method ($\Delta h^{m,m+1} = |h(DFAm) - h(DFAm+1)|$). For a DFA$m$, an m-order polynomial is used to calculate the local trend in each segment.

first is from 1951 to 1970; the second is from 1971 to 1990 and the third is from 1991 to 2010. In each synoptic station, the comparison of h^{orig}, h^{shuf}, and h^{surr} of rainfall from these three periods are done. This division was made considering the classification mentioned by some studies in West Africa [36–38]: 1951–1970 is considered as the wet period, 1971–1990 is the drought period, and 1991–2010 is the end of the drought.

2.2.5. Error Analysis of the DFA Exponents (h). To show the efficiency of the linear regression used to fit the fluctuation function in a log-log representation for determining the DFA exponents (h), Pearson coefficient is computed. To find out whether the straight line fitting to the fluctuation function in a log-log representation is statistically significant, we determine the confidence interval (lower and upper bound of the 95% confidence interval) for Pearson coefficient. The error analysis is done from the obtained values of the mean squared error (MSE).

3. Results

3.1. Long-Term Memory Characteristic Study. In the present study, we calculate the results for all the six synoptic stations

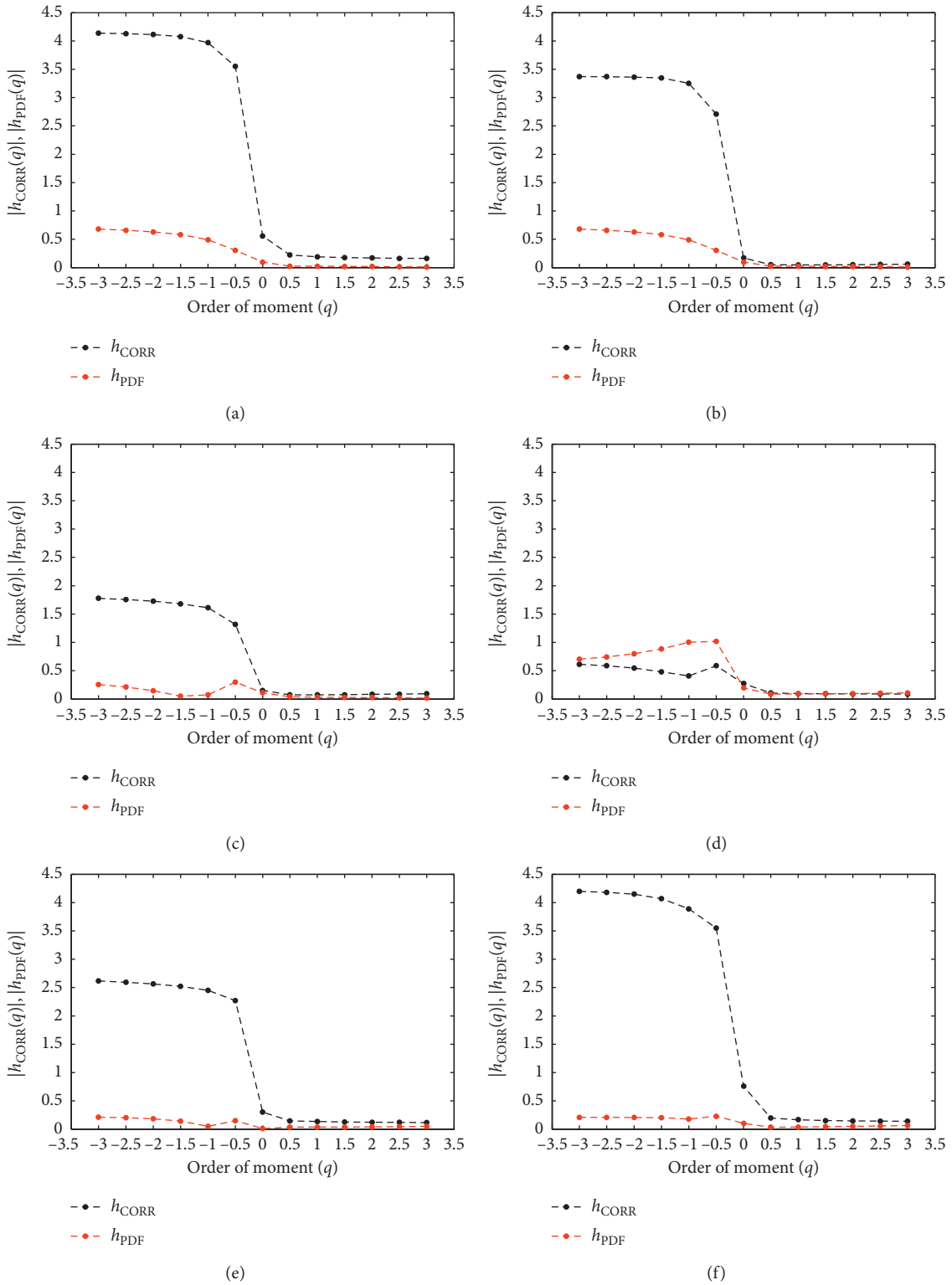

FIGURE 5: Absolute difference of Hurst exponents $|h_{CORR}(q)|$ and $|h_{PDF}(q)|$ as a function of (q) (where q) is the order of the fluctuation function), $q = -3 : 0.5 : 3$ at each synoptic station: (a) Cotonou station, (b) Bohicon station, (c) Savè station, (d) Parakou station, (e) Natitingou station, and (f) Kandi station.

in the range of 8–1024 days. Figure 3 shows South-North distribution of DFA exponent (h) obtained by the *DFA1-4* method. The main results of this figure are the following: (a) h values depend on the applied DFAm method; (b) except Cotonou, whatever the DFAm method, h values present spatial variation, there is a South-North gradient, (c) over all synoptic stations, h values are systematically between 0.5 and 1, this means that there exists positive long-term memory

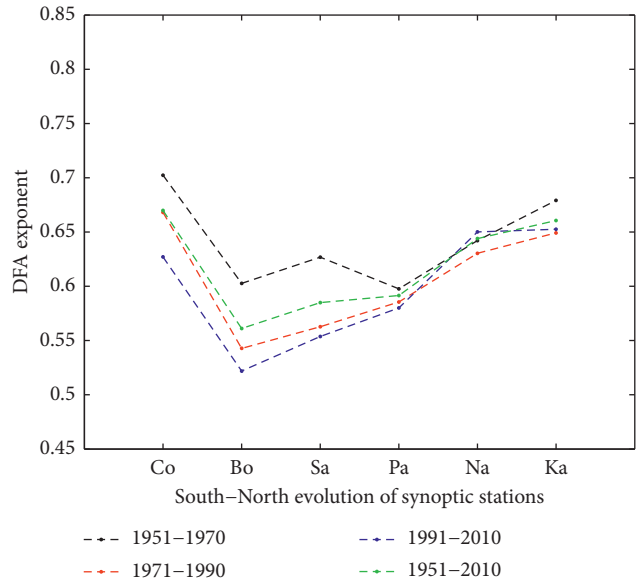

Figure 6: Spatiotemporal variation of DFA exponents (h) obtained by the *DFA2* method.

characteristic in the rainfall field, and (d) among synoptic stations, the highest and lowest values of h are, respectively, obtained at Cotonou and Bohicon stations, indicating the existence of strong and weak long-term memory characteristics in Cotonou and Bohicon.

3.2. The Best DFA Method. Figure 4 presents the South-North distribution of $\Delta h^{m,m+1}$ obtained for ($m = 1, 2$, and 3). It is observed that among *DFA1-4* methods, none is systematically the best over all synoptic stations. This result indicates that different kind of local trend exist in rainfall time series over Bénin. In addition, the *DFA1-4* method affects significantly and differently their multifractal characteristics. Thus, the best DFA method depends on the geographical position of the studied station. The comparison of the spatial average of $\Delta h^{m,m+1}$ (shown in Figure 4) reveals that *DFA2* minimizes $\Delta h^{m,m+1}$ spatially averaged among *DFA1-DFA4*. Therefore, *DFA2*, is adopted in the rest of this study.

3.3. Origins of Multifractality. Figure 5 shows the absolute difference of generalized Hurst scaling function obtained by *MFDFA2* corresponding to *DFA2* for original and shuffled data $|h^{\text{orig}}(q) - h^{\text{shuf}}(q)| = |h_{\text{CORR}}(q)|$ and original and surrogate data $|h^{\text{orig}}(q) - h^{\text{surr}}(q)| = |h_{\text{PDF}}(q)|$ as a function of q ($q = -3 : 0.5 : 3$) for the studied stations. The results reveal that in Bénin, excepted Parakou, at the synoptic station, the long-term temporal correlations are systematically the source of multifractality in rainfall.

3.4. Temporal Evolution of Long-Term Memory Characteristics. Figure 6 presents South-North distribution of DFA exponents (h) obtained over 1951–1970, 1971–1990, and 1991–2010 by the *DFA2* method. For all synoptic stations except Natitingou, $h_{[1951-1970]} < h_{[1971-1990]} < h_{[1991-2010]}$. This means that except Natitingou, the strength of long-term memory characteristic decreases each twenty years of the study period. The reason behind the exception done at Natitingou could be linked to the fact that Natitingou is the rainiest region of Bénin because of the presence of mountains (~800 m of high). However, DFA exponents are between 0.5 and 1 on each period. Thus, there exists positive long-term memory characteristics in the rainfall field at all stations on these periods.

3.5. Error Analysis of DFA Exponents (h). Figure 7 presents the latitudinal variation of Pearson coefficient for Hurst exponent for each subperiod. The results show that whatever the studied subperiod, the Hurst exponent is estimated by a Pearson coefficient greater than 97%, indicating the robustness of the linear regression used to fit the fluctuation function in a log-log representation.

The upper and the lower bound of the 95% confidence interval have the same sign meaning that the computation is statistically significant.

The error in the computation above for each subperiod is shown in Figure 8. One can remark that all the values of the MSE are lower than 8% showing a robustness of the computation process.

3.6. Assessment to Climate Change Effect by the DFA Method. The comparison of DFA exponents for original, shuffled, and surrogated data obtained over 1951–1970, 1971–1990, 1991–2010, and 1951–2010 is shown in Figure 9. For a good understanding of the results analysis, it is important to keep in mind that the red and black curves provide information on climatic and geographical influence, respectively. The analysis of results (shown by red curve) reveal the following: (1) In 1951–1970, considered as humid period in literature, the minimum and maximum values of DFA exponents are obtained at Savè and Natitingou stations. These findings could be explained by the fact that Savè is in the transitional zone

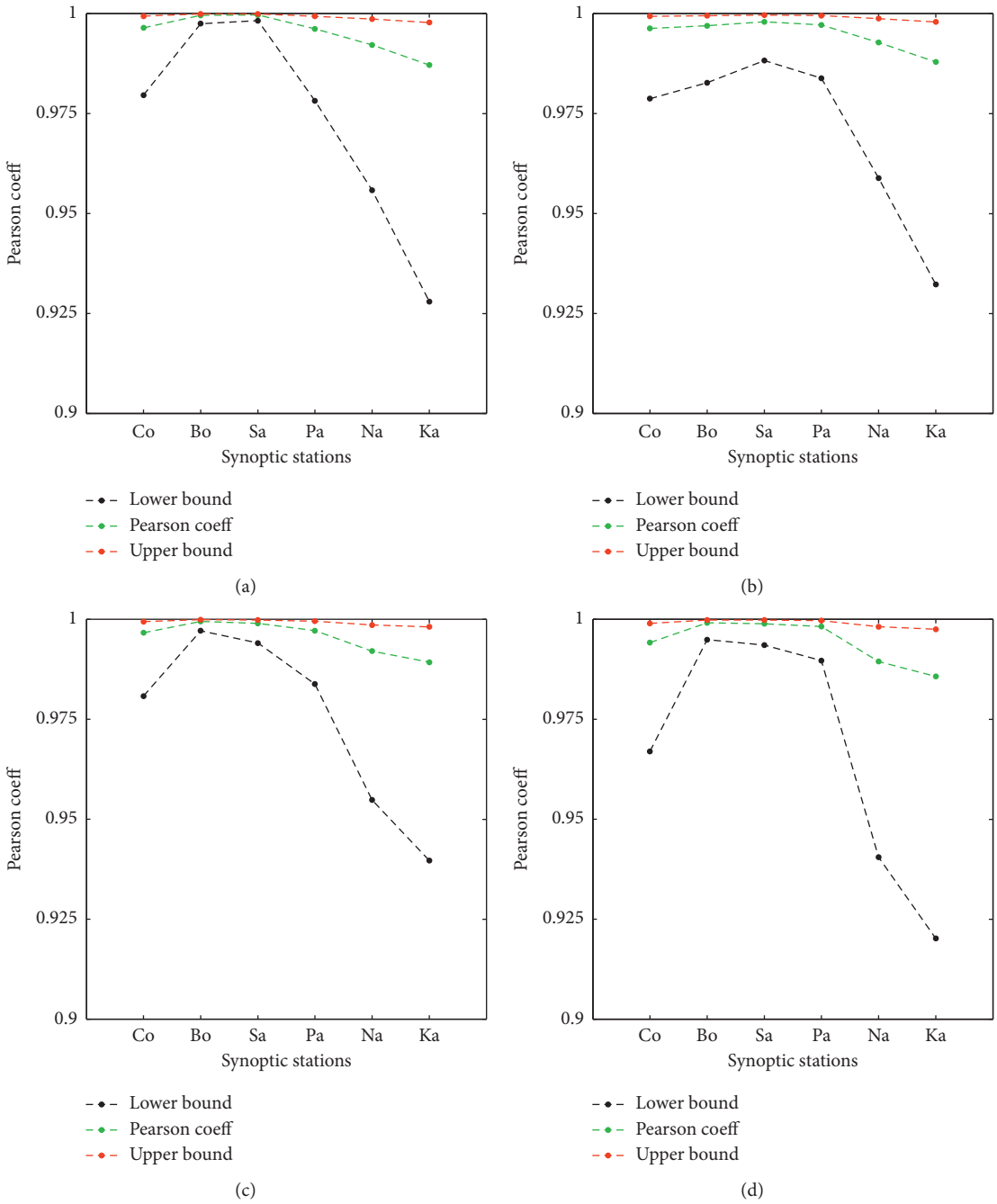

Figure 7: Spatiotemporal variation of Pearson coefficient for DFA exponent: (a) from 1951–2010, (b) from 1951–1970, (c) from 1971–1990, and (d) from 1991–2010. Red and black represent the upper bound and the lower bound of the 95% confidence interval. Green represents the Pearson coefficient.

between the Sudanian and subequatorial climates while Natitingou is in a mountainous area. Natitingou is therefore more watered, which is not surprising since Natitingou is known as the most watered area of Bénin. These results associated with the increasing of DFA exponents obtained and presented in blue curves at all stations confirm that 1951–1970 is a humid period. (2) In 1971–1990, considered as drought period in the literature, the transition zone is much more affected by drought, and this is noted by the greater values of h observed at Savè. The result confirms that a great drought has occurred during this subperiod. (3) In 1991–2010, considered as the end of the drought, it is observed that only the Natitingou station was actually watered, and this can be facilitated by the presence of mountains. However, no real recovery has been made in the other stations. Thus, in this period the, drought is still present in several regions of Bénin, and it is strongly severe in Savè and Parakou. These findings are confirmed by the randomly variation of DFA exponents over synoptic stations presented in blue curves, contrary to what is obtained by some authors in the literature for West

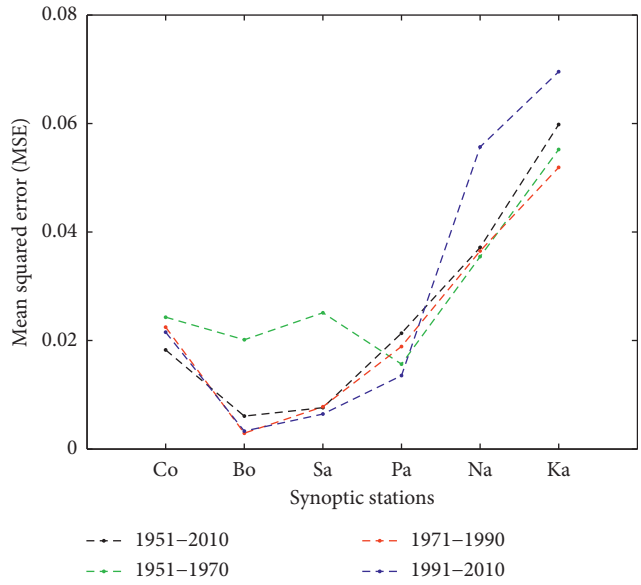

Figure 8: Spatiotemporal variation of the mean squared error (MSE).

Africa in general [36–38]. In the fractal approach, our results show that the subperiod 1991–2010 is not really a transition period, and the drought is prolonged until 2010. This result is not too surprising since there is some unanimity to date the onset of the drought episode around the 1970s, with the support of breakthrough statistical tests like that of Pettitt [39], there is a debate about its end [36].

4. Discussion

The obvious reasons behind the South-North gradient observed in Figure 3 except Cotonou may be explained by the fact that Bohicon is in the transition region between Sudanian and subequatorial region and Kandi is near to the Sahelian region. The highest values of h, obtained at Cotonou may be due firstly to the presence of Atlantic Ocean, which can affect Cotonou rainfall by their sea surface temperature and secondly to the anthropic effect created by the presence of many industries around.

The comparison of the spatial average of $\Delta h^{m,m+1}$ (shown in Figure 4) shows that $\text{mean}_{\Delta h^{2,3}} < \text{mean}_{\Delta h^{3,4}} < \text{mean}_{\Delta h^{1,2}}$; thus, *DFA2* minimizes $\Delta h^{m,m+1}$ spatially averaged among *DFA1-DFA4*. In Bénin, at the synoptic scale, *DFA2* is the best method in terms of spatial average. This result confirms those of [6, 24]. These authors have found the second-order DFA (*DFA2*) method as the best and the most commonly used order, respectively, for outgoing longwave and temperature records.

It is clearly observed in Figure 5 that, for all synoptic stations, for almost all values of q, with the exception of Parakou station, $|h_{\text{CORR}}(q)|$ is systematically larger than $|h_{\text{PDF}}(q)|$. This means that the effect of the broad probability density function on multifractality is more important in Parakou than that of long-term temporal correlations. Thus, in Bénin, except Parakou, at the synoptic station the long-term temporal correlations are systematically the source of multifractality in rainfall. Therefore, the source of multifractality in rainfall depends on the geographical position and the type of climate of the studied station. However, nonzero values of $|h_{\text{CORR}}(q)|$ and $|h_{\text{PDF}}(q)|$ indicate that both of them influence the multifractality. In specific cases, the long-range correlations have a slightly greater effect on rainfall multifractality than the broad probability density function, as $|h_{\text{PDF}}(q<0)| > |h_{\text{PDF}}(q>0)|$.

5. Conclusions

Traditional approaches cannot detect natural variability due to the dynamic behavior of climate variables. In this paper, the DFA method is used to analyze the long-term memory characteristic of rainfall over Bénin. The results reveal that over all synoptic stations, DFA exponent (h) is systematically between 0.5 and 1, meaning that there is a positive long-term memory characteristic in the rainfall field. However, among synoptic stations, highest and lowest values of h are, respectively, obtained at Cotonou and Bohicon stations, indicating strong and weak long-term memory characteristics in Cotonou and Bohicon. It is observed that among *DFA1-4* methods, none is systematically the best over all synoptic stations. This result indicates that different kinds of local trend exist in rainfall time series over Bénin. Thus, the best DFA method depends on the geographical position of the studied station. The comparison of the spatial average of Δh between two successive orders of DFA reveals that *DFA2* minimizes more Δh among *DFA1-DFA4*. Therefore, *DFA2* is considered as the best method and is used to calculate LTM in this study. For all stations, for almost all values of q, with the exception of Parakou station, $|h_{\text{CORR}}(q)|$ is larger than $|h_{\text{PDF}}(q)|$. This means that the effect of the broad probability density function on multifractality is more important than that of long-term temporal correlations, only for

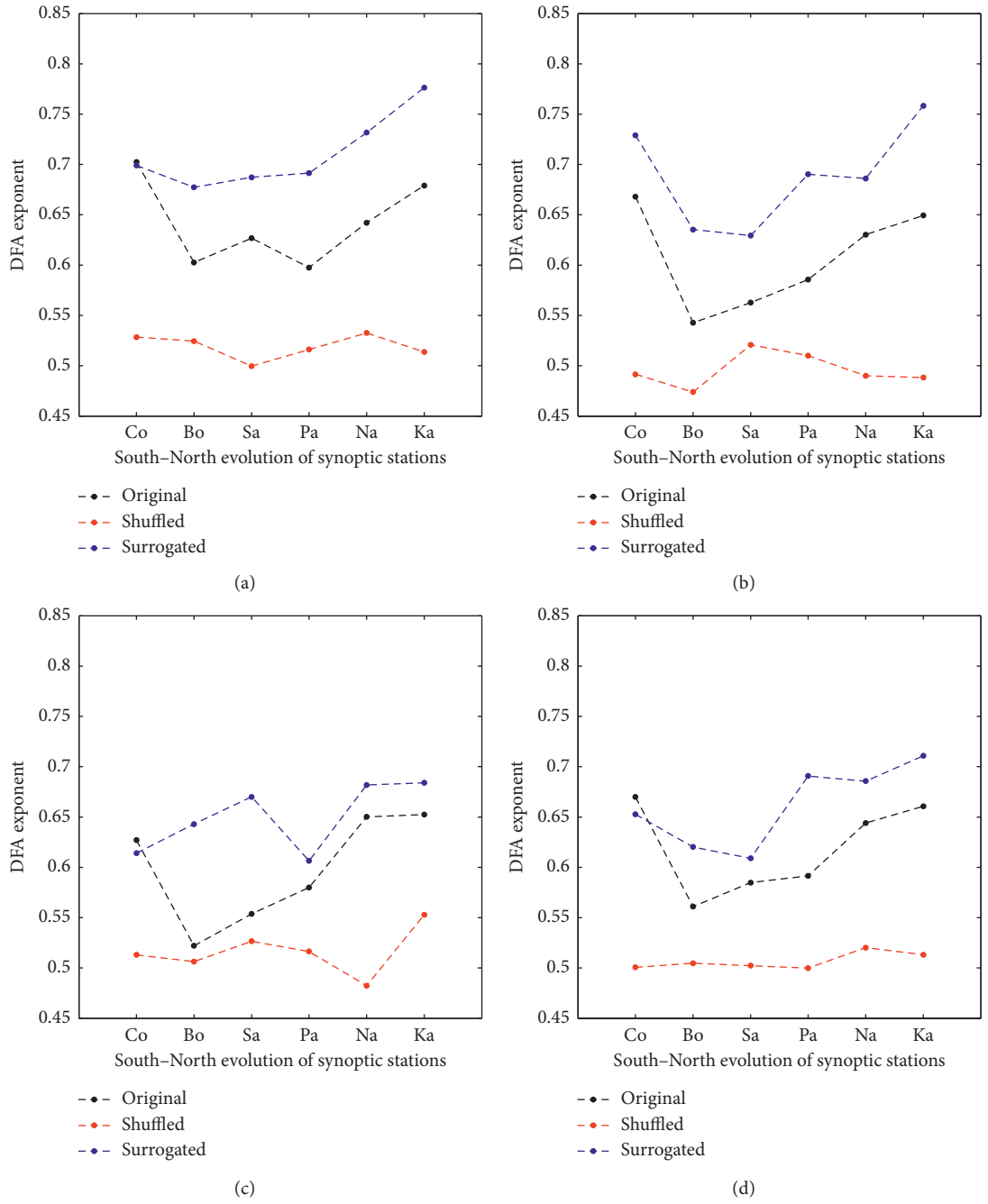

FIGURE 9: h^{orig} (black line), h^{shuf} (red line), and h^{surr} (blue line) for original, shuffled, and surrogated data obtained over 1951–1970 (a), 1971–1990 (b), 1991–2010 (c), and 1951–2010 (d).

Parakou. Thus, in Bénin, except Parakou, at the synoptic station, the long-term temporal correlations are systematically the source of multifractality in rainfall. However, nonzero values of $|h_{CORR}(q)|$ and $|h_{PDF}(q)|$ indicate that both broad probability density function and long-term temporal correlations influence the multifractality. Except Natitingou, the strength of long-term memory characteristic decreases each twenty years of the study period. In the fractal approach, our results show that the subperiod 1991–2010 is not really a transition period, and the drought is prolonged until 2010. Fractal theory is adapted to characterize Bénin climate. It should be good to confirm the existence of long-range correlations by studying the autocorrelation function (ACF) and the variability of the local slopes for large time scales as suggested in Maraun et al. [18] and clarified by Varotsos and Efstathiou [17]. These aspects of the analysis will be the objectives of future studies.

Data Availability

The precipitation data used in this study are supplied by the local service of ASCENA in Cotonou. The data are not

available online in any data base, so that we cannot provide a link to reach them. They are provided when researchers address request to ASCENA (http://www.ascena.aero).

Conflicts of Interest

The authors declare no conflicts of interest.

Acknowledgments

The authors would like to thank the Agency for the Safety of Air Navigation in Africa and Madagascar (ASECNA) for providing the data that we used to conduct this study.

Supplementary Materials

The precipitation data used to support the findings of this study are included within the supplementary information file(s). Please find attached the following files: (1) Precipitation data in the file box named (DATA). It contains six files. Each file represents each synoptic station data used (Cotonou, Bohicon, Savè, Parakou, Kandi, and Natitingou). (2) The Matlab programming codes used to study long-term memory characteristic, choose the best DFA method, find the origins of multifractality, illustrate the temporal evolution of long-term memory characteristics, and assess the climate change effect by the DFA method are presented in the file box named MATLAB_CODES. (*Supplementary Materials*)

References

[1] UNFCCC, *The United Nations Framework Convention on Climate Change (UNFCCC): report of the 12th Conference of the Parties (COP12) and the 2nd Meeting of the Parties (MOP2)*, United Nations Framework Convention on Climate Change (UNFCCC), United Nations Office, Nairobi, Gigiri, Kenya, November 2006, https://unfccc.int/resource/docs/2006/cop12.

[2] Intergovernmental Panel on Climate Change (IPCC), *Climate Change: Impacts, Adaptation and Vulnerability, Contribution of Working Group II to the Fourth Assessment Report of the Intergovernmental Panel on Climate Change*, Cambridge University Press, Cambridge, UK, 2007.

[3] B. Mondiale, *Inondation au Bénin: Rapport d'évaluation des Besoins Post Catastrophe*, Système des Nations Unies du Bénin, Benin, 2011.

[4] S. Pauleit, A. Coly, S. Fohlmeister et al., *Urban Vulnerability and Climate Change in Africa*, Springer, Vol. 4, Springer, Berlin, Germany, 2015.

[5] Z. Xu, Y. Tang, T. Connor, D. Li, Y. Li, and J. Liu, "Climate variability and trends at a national scale," *Scientific Reports*, vol. 7, no. 1, pp. 1–10, 2017.

[6] Z. Shen, J. Shi, and Y. Lei, "Comparison of the long-range climate memory in outgoing longwave radiation over the Tibetan Plateau and the Indian Monsoon Region," *Advances in Meteorology*, vol. 2017, Article ID 7637351, 7 pages, 2017.

[7] S. Solomon, D. Qin, M. Manning, Z. Chen, M. Marquis, and K. B. Averyt, "Technical summary," in *Climate Change 2007: The Physical Science Basis. Contribution of Working Group I to the Fourth Assessment Report of the Intergovernmental Panel on Climate Change*, pp. 19–92, Cambridge University Press, Cambridge, UK, 2007.

[8] X. Chen, G. X. Lin, and Z. T. Fu, "Long-range correlations in daily relative humidity fluctuations: a new index to characterize the climate regions over China," *Geophysical Research Letters*, vol. 34, no. 7, 2007.

[9] J. W. Kantelhardt, E. Koscielny-Bunde, D. Rybski, P. Braun, A. Bunde, and S. Havlin, "Long-term persistence and multifractality of precipitation and river runoff records," *Journal of Geophysical Research*, vol. 111, no. 1, pp. 1–13, 2006.

[10] Y. Zhou and Y. Leung, "Multifractal temporally weighted detrended fluctuation analysis and its application in the analysis of scaling behavior in temperature series," *Journal of Statistical Mechanics: Theory and Experiment*, vol. 2010, no. 6, article P06021, 2010.

[11] M. Luo, Y. Leung, Y. Zhou, and W. Zhang, "Scaling behaviors of global sea surface temperature," *Journal of Climate*, vol. 28, no. 8, pp. 3122–3132, 2015.

[12] M. N. Efstathiou and C. A. Varotsos, "Intrinsic properties of Sahel precipitation anomalies and rainfall," *Theoretical and Applied Climatology*, vol. 109, no. 3-4, pp. 627–633, 2012.

[13] M. S. Taqqu, V. Teverovsky, and W. Willinger, "Estimators for long-range dependence: an empirical study," *Fractals*, vol. 3, no. 4, pp. 785–798, 1995.

[14] M. S. Movahed, G. R. Jafari, F. Ghasemi, S. Rahvar, and M. R. R. Tabar, "Multifractal detrended fluctuation analysis of sunspot time series," *Journal of Statistical Mechanics: Theory and Experiment*, vol. 2006, no. 2, article P02003, 2006.

[15] M. S. Movahed and E. Hermanis, "Fractal analysis of river flow fluctuations," *Physica A: Statistical Mechanics and its Applications*, vol. 387, no. 4, pp. 915–932, 2008.

[16] C. M. Hall, "Complexity signatures for short time scales in the atmosphere above Adventdalen, Svalbard," *Journal of Geophysical Research: Atmospheres*, vol. 119, no. 2, pp. 652–662, 2014.

[17] C. A. Varotsos and M. N. Efstathiou, "On the wrong inference of long-range correlations in climate data; the case of the solar and volcanic forcing over the tropical pacific," *Theoretical and Applied Climatology*, vol. 128, no. 3-4, pp. 761–767, 2016.

[18] D. Maraun, H. W. Rust, and J. Timmer, "Tempting long-memory—on the interpretation of DFA results," *Nonlinear Processes in Geophysics*, vol. 11, no. 4, pp. 495–503, 2004.

[19] A. Kiraly and I. M. Janosi, "Detrended fluctuation analysis of daily temperature records: geographic dependence over Australia," *Meteorology and Atmospheric Physics*, vol. 88, no. 3-4, pp. 119–128, 2005.

[20] D. Rybski, A. Bunde, and H. von Storch, "Long-term memory in 1000-year simulated temperature records," *Journal of Geophysical Research*, vol. 113, no. 2, 2008.

[21] E. Koscielny-Bunde, A. Bunde, S. Havlin, H. E. Roman, Y. Goldreich, and H. J. Schellnhuber, "Indication of a universal persistence law governing atmospheric variability," *Physical Review Letters*, vol. 81, no. 3, pp. 729–732, 1998.

[22] A. Bunde, J. Kropp, and H. J. Schellnhuber, *The Science of Disaster: Climate Disruptions, Market Crashes, and Heart Attacks*, Springer, Berlin, Germany, 2002.

[23] M. Boko, "Climats et communautés rurales du bénin. Rythmes climatiques et rythmes de développement," Thèse de doctorat en Géographie, ABES, Paris, 1988.

[24] S. Wan, Q. Liu, J. Zou, and W. He, "Nonlinearity and fractal properties of climate change during the past 500 years in northwestern China," *Discrete Dynamics in Nature and Society*, vol. 2016, Article ID 4269431, 7 pages, 2016.

[25] L. Jiang, L. Zhao, and Z. Zhao, "On the difference of scaling properties for temperature and precipitation over China," *Advances in Meteorology*, vol. 2017, Article ID 5761275, 10 pages, 2017.

[26] J. W. Kantelhardt, S. A. Zschiegner, E. Koscielny-Bunde, S. Havlin, A. Bunde, and H. E. Stanley, "Multifractal detrended fluctuation analysis of nonstationary time series," *Physica A: Statistical Mechanics and Its Applications*, vol. 316, no. 1–4, pp. 87–114, 2002.

[27] L. Telesca, M. Balasco, G. Colangelo, V. Lapenna, and M. Macchiato, "Investigating the multifractal properties of geoelectrical signals measured in southern Italy," *Physics and Chemistry of the Earth, Parts A/B/C*, vol. 29, no. 4–9, pp. 295–303, 2004.

[28] K. Matia, Y. Ashkenazy, and H. E. Stanley, "Multifractal properties of price fluctuations of stocks and commodities," *Europhysics Letters (EPL)*, vol. 61, no. 3, pp. 422–428, 2003.

[29] R. Rak and P. Zieba, "Multifractal flexibly detrended fluctuation analysis," *Acta Physica Polonica B*, vol. 46, no. 10, p. 1925, 2015.

[30] J. Kwapien, P. Oswiecimka, and S. Drozdz, "Components of multifractality in high frequency stock returns," *Physica A: Statistical Mechanics and Its Applications*, vol. 350, no. 2–4, pp. 466–474, 2005.

[31] J. Theiler, B. Galdrikian, A. Longtin, S. Eubank, and D. J. Farmer, "Using surrogate data to detect nonlinearity in time series," in *Nonlinear Model, Forecast*, M. Casdagli and S. Eubank, Eds., pp. 163–188, Addison-Wesley, Redwood City, CA, USA, 1992.

[32] Q. Dong, Y. Wang, and P. Li, "Multifractal behavior of an air pollutant time series and the relevance to the predictability," *Environmental Pollution*, vol. 222, pp. 444–457, 2017.

[33] W. Hou, G. Feng, P. Yan, and S. Li, "Multifractal analysis of the drought area in seven large regions of China from 1961 to 2012," *Meteorology and Atmospheric Physics*, vol. 130, no. 4, pp. 459–471, 2018.

[34] J. Wang, P. Shang, and K. Dong, "Effect of linear and nonlinear filters on multifractal analysis," *Applied Mathematics and Computation*, vol. 224, pp. 337–345, 2013.

[35] E. A. Ihlen, "Introduction to multifractal detrended fluctuation analysis in matlab," *Frontiers in Physiology*, vol. 3, pp. 141–159, 2012.

[36] M. Balme, T. Lebel, and A. Amani, "Années sèches et années humides au sahel : quo vadismus?," *Hydrological Sciences Journal*, vol. 51, no. 2, pp. 254–271, 2004.

[37] P. Ozer, M. Erpicim, G. Demarée, and M. Vandiepenbeeck, "The Sahelian drought may have ended during the 1990s," *Hydrological Sciences Journal*, vol. 48, no. 3, pp. 489–492, 2003.

[38] D. Tapsoba, B. Bobee, L. Le Barbé et, and E. Elguero, "Quelques caractéristiques événementielles des régimes pluviométriques ponctuels ouest-africains au cours de deux périodes climatologiques contrastées (1951-1970 et 1971-1990)," *Sécheresse*, vol. 13, no. 2, pp. 95–104, 2002.

[39] A. N. Pettitt, "A non-parametric approach to the change-point problem," *Journal of Applied Statistics*, vol. 28, no. 2, pp. 126–135, 1979.